DIMMWIT
Comparing atmospheric seeing values measured by a Differential Image Motion Monitor, Which Is Transportable and COAST

B. O'Donovan[a], J.S. Young[a], P.J. Warner[a], D.F. Buscher[a], D.M. Wilson[a], R.C. Boysen[a], E.B. Seneta[a] and J.W. Keen[a]

[a]Mullard Radio Astronomy Observatory, Cavendish Laboratory, Cambridge, UK

ABSTRACT

The Cambridge DIMMWIT was developed for the site of COAST (the Cambridge Optical Aperture Synthesis Telescope), a prototype optical interferometer. Unlike other differential image motion monitors, this design is portable in order to carry out seeing campaigns at the site of any optical inteferometer. Of particular interest is the site of a second-generation interferometer proposed by the MRO (Magdalena Ridge Observatory) consortium. The DIMMWIT design has two objectives: to measure the Fried parameter r_0 and the speckle lifetime τ_0, and to be easily transportable. Here, we outline the theory of differential image motion, the design of the DIMMWIT, describe how turbulence parameters can be measured with COAST, and compare measurements of the seeing conditions made simultaneously by the monitor and COAST.

Keywords: site testing, seeing, interferometric

1. INTRODUCTION

How can the same monitor be used to carry out a seeing campaign at more than one site? Most seeing monitors are permanently installed and not easily transferred to another site. The aim of this project was to produce a seeing monitor capable of measuring the seeing conditions at any site around the world. This would be useful for finding the best site for an optical interferometer or for comparing the sites of existing interferometers. Extensive knowledge of the behaviour of the atmosphere at the site of a proposed interferometer would provide information about key design parameters such as operating wavelength, aperture size and coherent integration time.

Differential Image Motion Monitors (DIMMs) were developed to evaluate turbulent atmospheric conditions quantitively. The principle of differential image motion measurements is to allow light into an imaging system through two small apertures. The images from the two apertures are separated and their differential position over time is recorded. This method has two advantages. The system is insensitive to tracking errors,[1] as it is the relative motion of the images that is measured, and the instruments are compact because the distance between the apertures need only be a few times their diameter for the differential motion to dominate. Thus, DIMMs give an unbiased estimate of image degradation due to the atmosphere alone.

The prototype DIMMWIT developed in Cambridge can measure Fried's parameter. Further development will lead to measurements of the temporal coherence of the wavefronts. The design is limited by two conditions. The cycle time has to be short enough to estimate the coherence time, τ_0, which determines the choice of detector. In addition, the monitor must be easily transferred to another site, which determines the choice of telescope that is part of the monitor.

Section 2 reviews the theory of atmospheric turbulence and the resulting constraints on the DIMM design parameters. A description of the DIMM is given in section 3, followed by an outline of how the atmospheric parameters are found using COAST and using the DIMMWIT data. We then compare seeing estimates obtained with the instrument and with COAST to evaluate the performance of the DIMMWIT.

Further author information: (Send correspondence to B. O'Donovan)
B. O'Donovan.: E-mail: bo209@cam.ac.uk, Telephone: + 44 (0)1223 337247 Address: Mullard Radio Astronomy Observatory, Cavendish Laboratory, Madingley Road, Cambridge, CB3 0HE, UK

2. SPATIAL AND TEMPORAL BEHAVIOUR OF WAVEFRONTS

2.1. Physics of Turbulence and Fried's parameter

The atmosphere is made up of layers of air that have different temperatures and water vapour content.[2] These layers with different refractive indices are mixed together by turbulence, resulting in refractive index fluctuations in the atmosphere. The wavefronts of starlight are essentially 'flat' until these fluctuations introduce random phase delays in different parts of the wave, resulting in a distorted wave front, like a crumpled piece of paper.

Atmospheric air flow is nearly always turbulent. Air has a low kinematic viscosity, which means that the Reynolds number always exceeds the critical value of the structure, leading to fully developed turbulence. According to Kolmogorov, the kinetic energy of a turbulent flow is transferred from large scale motions to smaller and smaller scale motions. Once the Reynolds number becomes small enough, this process stops and the kinetic energy is dissipated by viscosity. It is assumed that viscous dissipation does not occur in the inertial range, between $1/L_0$ and $1/l_0$, where L_0 is the outer scale at which energy is injected into the system and l_0 is the inner scale where energy is dissipated. In this range, and assuming a near field approximation, the phase structure function (the mean squared differential phase difference between two points separated by a distance r in the aperture plane of a telescope) is

$$D_\phi =< |\phi(x) - \phi(x-r)|^2 >= 6.88(r/r_0)^{\frac{5}{3}}. \tag{1}$$

where r_0 is Fried's parameter. r_0 is defined as the critical pupil diameter under which the resolving power of a telescope is diffraction limited,[2] and it can also be interpreted as the region of the wave front over which phase perturbations are small.

2.2. Estimating Fried's parameter

Fried's parameter r_0 is related to the long exposure image size obtained with a large aperture by[3]

$$FWHM = 0.98\lambda/r_0. \tag{2}$$

However, this single aperture technique is sensitive to telescope shake and tracking errors, from which atmospheric perturbations cannot be distinguished.

With the differential method, images from two apertures (usually on a common mount) are separated. By recording the differential position of the two images over time, tracking errors are eliminated. Telescope vibrations affect the two images in the same way, while turbulence causes small differential movements of the images.[1] In this way, the phase perturbations can be derived from variations in the separation of the images. The variance of the image motion parallel and perpendicular to the direction of separation of the apertures can be derived from the phase structure function[1]:

$$\sigma_l^2 = 2\lambda^2 r_0^{\frac{5}{3}}[0.179D^{-\frac{1}{3}} - 0.0968d^{-\frac{1}{3}}], \tag{3}$$

$$\sigma_t^2 = 2\lambda^2 r_0^{\frac{5}{3}}[0.179D^{-\frac{1}{3}} - 0.145d^{-\frac{1}{3}}], \tag{4}$$

where D is the diameter of the sub-apertures and d is the separation of the centres of the apertures. Using these expressions gives two estimates for r_0, which should agree. There is the added advantage of reducing the statistical error by taking an average of the two results.

2.3. Temporal characteristics of wavefronts

Another parameter τ_0 is introduced to describe the temporal behaviour of the wavefront. τ_0 is the correlation or coherence time and it is derived from Taylor's hypothesis that the behaviour of the atmosphere can be modelled as a frozen pattern of length r_0 being blown past the telescope in a time τ_0.[2] If v is the velocity at which such 'frozen turbulence' is blown past the telescope by the wind, then τ_0 is simply r_0/v.

3. DESCRIPTION OF PROTOTYPE DIMMWIT

For simplicity, the main components of the prototype DIMMWIT are a mask, telescope and CCD controlled by a computer, as shown in figure 1. The aperture mask has two apertures of variable separation and diameter, but most measurements are made with 8cm apertures separated by 25cm. The optical system is a Schmidt-Cassegrain telescope on an equatorial mount, with an aperture of 14 inches (356 mm) and a focal length of 3910 mm. The telescope drive system corrects the position of the telescope every second in order to track a target. There were two models of CCD camera used as part of the prototype to record the image positions. The S-BIG ST-5C camera has 10micron square pixels in an array of 320 x 240 pixels. The MX516 has an array of 550 by 290 pixels and the pixel size is 9.8 by 12.6 microns. In both cases, the CCD head was directly mounted at the prime focus of the telescope into an eyepiece holder.

Figure 1. Prototype DIMMWIT with Schmidt-Cassegrain 14" telescope

The 14" telescope is permanently installed at the site and must be polar aligned at the beginning of the night. The better the alignment the better the telescope tracks the targets. The system operates in two modes. One measures the FWHM of a long exposure image and the other is the DIMM mode. In the first mode, the telescope is focused and the focal length is measured by recording several images of a binary star of separation ∼10". A series of long exposure (1 second) images captured with the telescope pointing at a chosen target. In the DIMM mode, a mask is attached and the telescope is defocused by a small amount. The new focal length has to be measured by observing a binary star of separation ∼20". DIMM measurements of a brighter target can then be made once the telescope has been manually adjusted so that the image falls on the section of the CCD array near the readout register. The DIMM measurements are repeated several times before moving onto a new target, in order to measure the atmospheric conditions in another part of the sky. If possible, measurements of each target are made in both modes. The observer has to be present to initiate capture of a new series of images, after manually adjusting the telescope to keep the image near the readout register, and to point the telescope at a new target. The images are captured by the CCD camera and stored for later analysis.

As was stated in section 1, the design of the DIMMWIT is limited by two conditions. The first is that the cycle time has to be short enough to estimate the coherence time, τ_0, which is of the order of milliseconds. By cycle time, we mean the time between successive images - the exposure time and download time of the CCD. Finding a commercial CCD capable of short cycle times is difficult. The first camera tested was the ST-5C camera, which is supported by commercial software. Downloading a subframe of the array takes less time than downloading the entire array. Hence, faster download times are achieved by selecting a subframe of the array around the images to download. The shortest exposure time of the camera is 10ms. The download time from the controller to the host PC takes between 0.5 and 1 second, resulting in a total cycle time of the order of seconds. So, the camera can be used to make measurements of r_0 but the cycle time is too long for measurements of

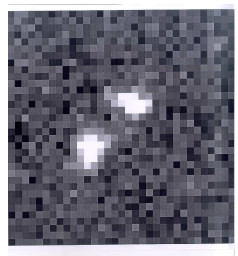

Figure 2. Typical image taken with SBIG CCD showing the two spots obtained by defocusing the telescope.

τ_0. For this reason, another CCD, by Starlight X-press, was chosen. Customised software has been written to control the camera for exposure times as short as 1ms and to download a subframe near the readout register in a few ms. Hence, the total cycle time of the system is of the order of ms, provided the subframe is near the readout register.

The second condition of the design was that the monitor had to be transportable. With the present choice of telescope, the prototype does not appear to be portable. However, if there is a large amateur telescope, 12 or 14 inches in diameter, available at the site to be studied, a new mask and the CCD can be attached to make a DIMM. The other choice of telescope is a small telescope, 5 inches in diameter, to which additional optics are added to allow aperture separations greater than the telescope diameter. This telescope would be small enough to be 'luggage' and thus taken to any site where no other telescope was available. The important property of the telescope chosen is its ability to track a target accurately. The images must remain near the readout register of the CCD during all measurements to obtain the cycle times quoted above. The telescope used must therefore have an autoguider port to receive an autoguiding signal.

4. MEASUREMENT OF SEEING PARAMETERS WITH COAST

The seeing parameters can be estimated from interference fringes recorded by COAST. The coherence time is the length of time over which the fringes remain coherent.[4] Fried's parameter, r_0 is estimated from the visibility amplitudes of the interference fringes. A turbulent atmosphere, obeying Kolmogorov statistics, is simulated. Visibilities for different aperture diameters and wavelengths can be compared to simulated values in order to calculate Fried's parameter, r_0.

When COAST observes a star, the path travelled by the light in each beam is equalized and the beams are then passed to a beam combiner. By sweeping the path compensation trolleys back and forth, the optical path of one or more of the beams is modulated before combination, generating temporally encoded interference fringes. The fringes are recorded by measuring the time-varying intensity at each output of the beam combiner. The coherence time is inversely proportional to the width of the fringe peak in the power spectrum of the intensity patterns recorded.

Fried's parameter r_0 can be estimated from the visibility amplitudes calculated from the recorded COAST files. Recording four beam combiner outputs of varying aperture size (d) and filter (λ) gives four simultaneous visibility measurements. Assuming an initial value of r_0 for a standard wavelength, λ_o, (the central wavelength of one of the filters), each visibility corresponds to a value of d/r_0. How well the measured visibilities fit the simulated visibilities is given by a chi-squared value. The value of r_0 is adjusted until χ^2 is a minimum. This final value is our estimation of $r_0(\lambda_o)$.

How were the wavelengths and aperture sizes selected? Visibilities are not only reduced by the effect of the atmosphere. They are also affected by the instrumentation. For example, misalignments in the beam combiner will reduce the visibilities. Instrumental and atmospheric effects are both functions of wavelength and aperture size. How can we distinguish the reduction due to the atmosphere from that due to instrumentation? For long wavelengths and small aperture sizes, the reduction due to the instrument should be small. Therefore, by selecting long λ and small d, we hope that the instrumentation will not affect our measurements adversely.

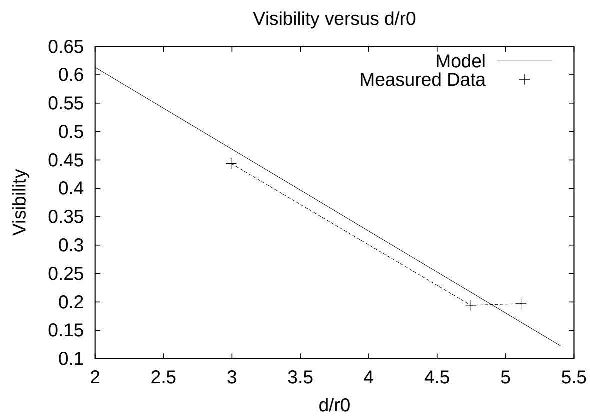

Figure 3. Best fit (r_0=3.82 cm at λ=905 nm) between predicted and measured visibilities for measurements made on 14.08.02. There are only three measured data points, as one of the APD's was inoperable at the time of measurement.

Predicted visibility amplitudes for different values of d/r_0 are calculated using a simulation[5] of a turbulent atmosphere obeying Kolmogorov statistics. Several assumptions are made: the intensity of the light incident on the apertures is equal and the optical throughput from both apertures is identical. The tilt component of the wavefront perturbations is compensated by a simulated fast autoguider. A guider with a fixed delay δt is simulated by using the tilt correction signal derived from a patch of turbulence offset by vδt from the patch of turbulence used to derive the interferometric signal. The guider delay is related to the total cycle time of the autoguider at COAST, in units of the coherence time τ_0. For simplicity, a linear fit is applied to the simulated visibilities. Figure 4 shows that a linear fit is acceptable for our analysis.

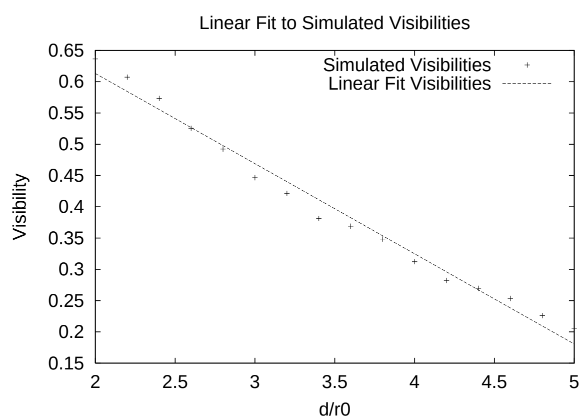

Figure 4. Simulated visibilities with a guider delay set to 0.15τ_0. A linear fit is then applied.

Certain assumptions are made in order to calculate visibility amplitudes from COAST data: the beam combiner is perfectly aligned, the intensities of the interfered beams are equal and the filter has an infinite bandpass.[4] Normally, it does not matter if these assumptions are correct, as the visibilities are calibrated, and so the effect of these assumptions cancel out. Here however, we are interested in the uncalibrated visibilities, so several corrections need to be made. First, the effect of using a filter with a finite bandpass must be taken into account. Due to the filter the fringes lie within a fringe envelope, which leads to a reduction in the total power contained in one sweep of the trolley. The idealised shape of the filter is used to simulate observing with no atmosphere. The ratio of the total power in a power spectrum without a filter over the total power in the idealised spectrum is calculated. This correction factor can then be applied to the visibilities. Secondly, the simulated visibilities assumed that the intensities of the two beams before combination were equal. However, the beams have different intensities due to instrumentation, so the simulated visibilities need to be adjusted.

Finally, we need to calculate the error in estimating r_0 by this method. Each visibility Y_k has an error of σ_k and is measured at an aperture diameter d_k and a wavelength λ_o. We fit the set of four measured visibilities Y_k to the set of visibilities y_k given by

$$y_k = mx_k + c, \quad \text{where} \quad x_k = \frac{d_k}{r_0(\lambda_k)} = \frac{d_k}{r_0(\lambda_o)\left(\frac{\lambda_k}{\lambda_o}\right)^{\frac{6}{5}}}. \tag{5}$$

χ^2 (see equation 6) is a minimum for the best fit between the measured visibilities and the linear equation. The value of $r_0(\lambda_o)$ at this minimum is our estimate of Fried's parameter. The error of our estimate comes from the width of the minimum of χ^2.[6]

$$\chi^2 = \frac{1}{N-1}\sum \frac{(mx_k + \mathrm{c} - Y_k)^2}{\sigma_k^2}. \tag{6}$$

5. RESULTS: ANALYSIS AND COMPARISONS

5.1. Determination of r_0 from DIMMWIT measurements made on 14th August 2002

Due to adverse weather conditions, most nights where the seeing was acceptable were used to debug the system. Here, we present measurements taken on one night, where the COAST array was available to take seeing measurements simultaneously. For each measurement of r_0 with the DIMM, 200 consecutive images are captured and the centroid positions are calculated using a barycentre algorithm.[3] The co-ordinates are transferred to axes parallel and perpendicular to the mean separation of the two images so that r_0 can be computed from equations 3 and 4. A plot of transverse versus longitudinal components of r_0 is shown in figure 5. From the few acceptable measurements made we can see that the transverse and longitudinal values do not always agree as expected. It is for this reason that it is advised[1] to calculate both components as a means of debugging the system. Obviously, further improvements could be made to the system so that the slope of the regression line is 1 with a spread of 5% (see below).

Fried's parameter, r_0, is a function of the variance of the differential position in radians. Hence, measuring the focal length of the system and calculating the variance of the differential position in pixels are the two sources of error, so that

$$\left(\frac{\delta r_0}{r_0}\right)^2 = \left(\frac{\delta\sigma^2}{\sigma^2}\right)^2 = \left(\frac{\delta\sigma_p^2}{\sigma_p^2}\right)^2 + \left(\frac{\delta f}{f}\right)^2. \tag{7}$$

where σ^2 is the variance of the differential position in either direction (longitudinal or transverse) in radians with error $\delta\sigma^2$, σ_p^2 is the variation in the focal place in metres with error $\delta\sigma_p^2$, and f is the measured focal length of the optical system with error δf. The error in measuring the separation of the binary stars leads to a 5% error in focal length measurement.

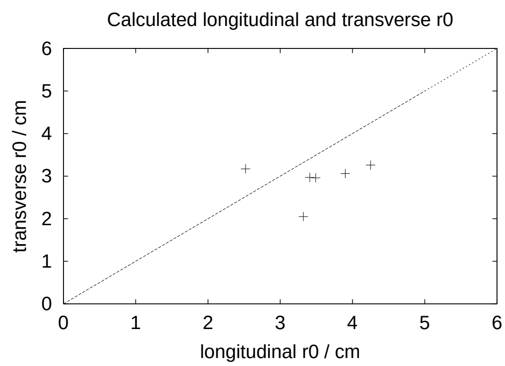

Figure 5. Comparing transverse and longitudinal values of Fried's parameter r_0 measured on 14/08/02 with the SBIG camera (λ_{eff}=639 nm).

Errors in the centroid co-ordinates and statistical errors contribute to $\delta\sigma^2$. The accuracy in determining the centroid of the image is limited by the photon noise and the readout noise of the CCD. If the photon noise and readout noise is approximated as a Poisson distribution, then the centroiding error of a Gaussian spot is[7]

$$\sigma_c = \frac{4\sigma_r}{\sqrt{3}G_s N_s (\frac{N_t}{N_s})^3} \times \frac{\lambda}{2\pi d}. \tag{8}$$

Here σ_c is the one-dimensional rms error of the centroid position, σ_r is the rms readout noise per pixel ($25e^-$), G_s is the peak count per pixel ($1400e^-$), N_s is the width of the region used for centroiding (4 pixel), N_t is the FWHM of the spot (2 pixel), λ is the operating wavelength (640nm) and d is the subaperture size (8cm). For these values we obtain a rms error of 0.02 of a CCD pixel.

Statistical errors occur because we calculate σ^2 from N short exposure images. If the atmosphere's statistical properties remain constant in the time it takes to record 200 images then $\delta\sigma^2$ is given by[1]

$$\frac{\delta\sigma_*^2}{\sigma_*^2} = \sqrt{\frac{2}{N-1}}. \qquad * = t, l \tag{9}$$

For measurements taken with the SBIG camera, we are assuming that the atmosphere does not change over several minutes.

Knowing the amount of error in all our measurements leads to a calculation of 5% error in our estimate of r_0. This is the percentage quoted above for the results in figure 5. However, the effective wavelength of the detector used to make the the measurements is (639 ± 15) nm, and we wish to present our results at a standard of 500 nm. Fried's parameter is a function of wavelength, $r_0 \propto \lambda^{\frac{6}{5}}$, so the new error is given by

$$\left(\frac{\delta r_0(\lambda_1)}{r_0(\lambda_1)}\right)^2 = \left(\frac{\delta r_0(\lambda_0)}{r_0(\lambda_0)}\right)^2 + \left(\frac{6}{5}\right)^2 \left(\frac{\delta\lambda_0}{\lambda_0}\right)^2. \tag{10}$$

where λ_1 is the new wavelength and λ_0 is the old wavelength of 639 nm.

In the determination of the effective wavelength of the CCD, it is assumed that the target star Vega can be approximated as a blackbody source of temperature 10,000 K, that the transmission function of the atmosphere is flat and that the quantum efficiency can be read accurately from the response curve sent with the CCD. The error in reading the quantum efficiencies was determined to have a negligible effect on the effective wavelength. The effect of approximating the target as a blackbody source introduced a 2% error to our estimation of the effective wavelength. The effect of assuming a flat atmospheric transmission function was not quantified. Therefore, the total error in our scaled value of Fried's parameter is 6%.

5.2. Comparing COAST and prototype DIMM data 14.08.02

Measurements made with COAST at λ=500nm: The values have been scaled in a similar manner to that outlined in section 5.

$$r_0 = 1.9 \pm 0.1\text{cm} \tag{11}$$

$$\tau_0 = 4.9 \pm 0.3\text{ms} \tag{12}$$

Measurements made with prototype DIMMWIT at 500 nm in single aperture mode (13) and DIMM mode (14).

$$r_0 = 2.1 \pm 0.1\text{cm for long exposures of 1 second} \tag{13}$$

$$r_0 = 2.38 \pm 0.15\text{cm for short exposures of 10 ms} \tag{14}$$

First, we compare the estimates of Fried's parameter, r_0. The COAST measurement gives the lowest expected value of r_0. Misalignments in the instrumentation, for example, might mean that Fried's parameter actually has a much higher value. Using the DIMM in single aperture mode is also useful for a lower limit on the expected value of r_0. Our final estimate of r_0 is a value of about 2.38 cm. The results imply that the performance of the DIMMWIT is acceptable. Some might find such an estimate of r_0 surprising, but seeing conditions of 2 cm have been recorded at other sites. Measurements of Fried's parameter have not been made at the site of COAST before. At 830 nm, the coherence time would be about 9 ms, which is a typical value recorded at COAST.[8] If the two seeing parameters are correlated, such 'bad' seeing conditions at COAST are expected to occur frequently. (The shortest r_0 recorded so far at the MRO site is 5.8 cm).

What are the shortest coherence times that the DIMMWIT will need to measure? If we scale the coherence time to represent τ_0 at the operating wavelength of the new Starlight X-press camera, which is 525nm, we get 5 ms. And we know from COAST data that τ_0 is often between 3 and 4 ms at this wavelength,[8] and it can be as short as 2 ms. The aim is for the DIMMWIT to be able to measure coherence times of the order of 4 ms, as the interferometers are unlikely to operate well at coherence times shorter than this.

6. CONCLUSION

Further measurements of Fried's parameter need to be made with the DIMMWIT and COAST before the performance of the DIMMWIT can be judged to be satisfactory. The next important step is to be able to measure the coherence time τ_0. This capability requires more development of the customised software for the MX516 CCD. Also, the tracking system of the chosen telescope must keep the images in a 32 by 16 region near the readout register of the CCD so that the cycle times are of the order of 4 ms. Hence, the images can be recorded in quick enough succession to calculate the wind speed from a cross-correlation of the differential positions. With the new CCD and telescope, measurements of the coherence time should be possible.

ACKNOWLEDGMENTS

Thanks to those at Mullard Radio Astronomy Observatory, Cambridge for their contributions.

REFERENCES

1. M. Sarazin and F. Roddier, "The ESO differential image motion monitor," *Astron. Astrophys.* **227**, pp. 294–300, 1990.
2. B. Lopez and M. Sarazin, "The ESO atmospheric temporal coherence monitor dedicated to high angular resolution imaging," *Astron. Astrophys.* **276**, pp. 320–326, 1993.
3. J. Vernin, "Measuring Astronomical Seeing: The DA/IAC DIMM," *Pub. Astron. Soc. Pac.* **107**, pp. 265–272, 1995.
4. D. Burns, *Experiments with the Cambridge Optical Aperture Synthesis Telescope*, PhD Thesis, University of Cambridge, 1997.
5. J. W. Keen, D. F. Buscher, and P. J. Warner, "Numerical simulations of pinhole and single-mode fibre spatial filters for optical interferometers," *Mon. Not. R. Astron. Soc.* **326**, pp. 1381–1386, 2001.
6. D. S. Sivia, *Data Analysis: A Bayesian Tutorial*, Clarendon Press, Oxford, 1996.
7. D. St-Jacques, G. C. Cox, J. E. Baldwin, C. D. Mackay, E. M. Waldram, and R. W. Wilson, "The JOSE atmospheric seeing monitor at the William Herschel Telescope," *Mon. Not. R. Astron. Soc.* **290**, pp. 66–74, 1997.
8. J. E. Baldwin, "Current Status of COAST," in *Astronomical Interferometry*, R. D. Reasenberg, ed., *Proc. SPIE* **3350**, pp. 736–746, 1998.